

Shell-model description for the first-forbidden β^- decay of ^{207}Hg into the one-proton-hole nucleus ^{207}Tl

Anil Kumar, Praveen C. Srivastava

Department of Physics, Indian Institute of Technology Roorkee, Roorkee 247667, India

Abstract

In this work, we have performed large-scale shell-model calculations for the first-forbidden β^- decay of ^{207}Hg into the one-proton-hole nucleus ^{207}Tl corresponding to the recently available experimental data from ISOLDE-CERN [T. A. Berry *et al.*, Phys. Rev. C 101, 054311 (2020)]. We have used the one-particle one-hole ($1p-1h$) truncation for both protons and neutrons simultaneously across the doubly-shell closure at ^{208}Pb in the final states of ^{207}Tl . In our calculations, we have also considered the effect of mesonic enhancement $\epsilon_{\text{mec}} = 2.01 \pm 0.05$ in the rank-0 for the axial-charge matrix element γ_5 . Here, we have calculated the $\log ft$ values from the ground-state of ^{207}Hg to the several excited states of ^{207}Tl and obtained a good agreement between the calculated and the experimental data. In the experimental data spin and parity for some states are not yet confirmed, thus based on the shell-model results for the $\log ft$ values we have given the prediction for these states. This is the first theoretical calculation for the $\log ft$ values for these transitions.

Keywords: Shell-model, First-forbidden beta decay

1. Introduction

In the recent past, several experiments have been performed to study the structure including collectivity and β decay properties in the lead region. In this

Email addresses: akumar5@ph.iitr.ac.in (Anil Kumar),
praveen.srivastava@ph.iitr.ac.in (Praveen C. Srivastava)

region, the low-lying states are characterized by the single-particle structures, while the higher energy states are due to core breaking. The first excited 3^- state in ^{208}Pb is highly mixed and has complex wave function [1, 2]. Wilson et al. [3] have measured the high-spin states above the 3.813 MeV in the nucleus ^{207}Tl and also they have reported the shell-model results corresponding to $t = 1$ truncation (where t is the number of nucleons excitation across the ^{208}Pb core) for both protons and neutrons. After that, the same group measured the new excited states in ^{207}Tl through the β^- decay of ^{207}Hg in the energy range of 2.6-4.0 MeV [4]. In these experiments, several new excited states have been identified in ^{207}Tl . The high-precision β spectrum of the first-forbidden nonunique β^- decay of ^{210}Bi has been measured in Ref. [5]. The experimental evidence for competition between allowed and first-forbidden β decay in the case of $^{208}\text{Hg} \rightarrow ^{208}\text{Tl}$ to understand the mechanism in the rapid neutron capture process is reported in Ref. [6]. The aims of these experiments are to study structure, beta decay properties, and astrophysical processes.

Theoretical study for the first-forbidden β decay in the lead region assessed by the shell-model with the phenomenological interactions are available in the literature [7, 8, 9, 10, 11, 12]. The first-forbidden β^- decay of $^{206}\text{Tl}(0^-) \rightarrow ^{206}\text{Pb}(0^+)$ in the framework of the shell-model was reported in Ref. [7] by considering the core polarization effect. In this work, they have found that the large quenching is needed in the couplings constants. A more comprehensive study of the first-forbidden β decay of the mass number $A = 205 - 212$ around the doubly magic nucleus ^{208}Pb was performed by Warburton [8] and extracted the large mesonic enhancement factor $\epsilon_{\text{mec}} = 2.01 \pm 0.05$ in the rank-zero matrix element of γ_5 . In Ref. [10] the Gamow-Teller and first-forbidden transitions were taken into account to calculate the half-lives of the isotones with the neutron magic number of $N = 126$. It was concluded that the first-forbidden transitions are important to reduce the half-lives in the study of the r -process including those besides the supernova explosions. In Ref. [11], the study of the first-forbidden contributions for the r -process waiting-point nuclei at the magic neutron numbers $N = 50, 82, \text{ and } 126$ were reported using the large

scale shell-model calculations and also found that the large quenching factor is needed in the coupling constants in the lead region. The high-precision theoretical β spectrum for the ground-state-to-ground-state first-forbidden transitions of $^{212,214}\text{Pb}$ that are relevant to the background of liquid xenon dark matter detectors are reported in Ref. [12]. The structure of ^{208}Po populated through EC/ β^+ decay of ^{208}At is reported in Ref. [13].

Recently, an experiment has been performed to study the β^- decay of ^{207}Hg into the ^{207}Tl through γ -ray spectroscopy at ISOLDE-CERN [4]. In this experiment, they have observed several new excited states and β feeding branching ratio between the energy range 2.6-4.0 MeV for ^{207}Tl through β^- decay of ^{207}Hg . In this work [4] shell-model results for the energy spectra using KHM3Y interaction have been reported, although, no shell-model results for the $\log ft$ values are reported. These new data motivated us to perform large scale shell-model calculations for the $\log ft$ values corresponding to β^- decay of $^{207}\text{Hg}(9/2_{\text{g.s.}}^+) \rightarrow ^{207}\text{Tl}(J_f^\pi)$ transitions. To the best of our knowledge, there is no theoretical calculations are available for these transitions in the literature. In the present study, we have made $1p$ - $1h$ excitations simultaneously for both protons and neutrons in the final states across the doubly-shell closure ^{208}Pb suggested by Warburton in Refs. [7, 8, 9]. The first-order contributions from nucleon excitations across the core can significantly affect the first-forbidden nuclear matrix elements [7]. In this work, we have adopted the large quenching in the weak coupling constants, also the mesonic enhancement factor $\epsilon_{\text{mec}} = 2.01 \pm 0.05$ [8, 9] in the rank-0 axial-charge matrix element γ_5 corresponding to $\Delta J = 0$ transitions. The present study will add more information to Berry et al. [4] work.

This paper is organized as follows. In Sec. 2, we give a short overview of the formalism for the forbidden β^- decay. Results and discussions about the interactions and β decay rate calculations are presented in the Sec. 3. Finally, in Sec. 4 we give summary and conclusions.

2. β -decay theory

The partial half-life of the β decay process can be expressed as [14, 15]

$$t_{1/2} = \frac{\kappa}{\tilde{C}}, \quad (1)$$

where κ is the constant and has the value [16]

$$\kappa = \frac{2\pi^3 \hbar^7 \ln(2)}{m_e^5 c^4 (G_F \cos\theta_C)^2} = 6289 \text{ s}, \quad (2)$$

where the θ_C is the Cabibbo angle. The \tilde{C} is the dimensionless integrated shape function which is defined as

$$\tilde{C} = \int_1^{w_0} C(w_e) p w_e (w_0 - w_e)^2 F_0(Z, w_e) dw_e. \quad (3)$$

Where the w_0 is the end-point energy, w_e and p_e are the total energy and momentum of the emitted electrons, respectively, and the factor $F_0(Z, w_e)$ is the Fermi function. The $C(w_e)$ is the shape factor, which contains all the nuclear structure information about the β decay transitions. To calculate the ft -values, we have multiplied the partial half-life with the following dimensionless integrated Fermi function

$$f_0 = \int_1^{w_0} p w_e (w_0 - w_e)^2 F_0(Z, w_e) dw_e, \quad (4)$$

and the $\log ft$ value is calculated by

$$\log ft = \log_{10}(f_0 t_{1/2} [s]). \quad (5)$$

The general form of the shape factor $C(w_e)$ in Eq. 3 can be expressed as

$$C(w_e) = \sum_{k_e, k_\nu, K} \lambda_{k_e} \left[M_K(k_e, k_\nu)^2 + m_K(k_e, k_\nu)^2 - \frac{2\gamma_{k_e}}{k_e w_e} M_K(k_e, k_\nu) m_K(k_e, k_\nu) \right],$$

where the K is the order of forbiddenness for β decay, the indices k_e and k_ν ($k_e, k_\nu = 1, 2, 3, \dots$) are the positive integers that emerged from the partial wave expansion of the leptonic wave functions. Here the auxiliary quantities are $\gamma_{k_e} = \sqrt{k_e^2 - (\alpha Z)^2}$ and $\lambda_{k_e} = F_{k_e-1}(Z, w_e)/F_0(Z, w_e)$, where the λ_{k_e} is the Coulomb function and $F_{k_e-1}(Z, w_e)$ is the generalized Fermi function [17, 14,

18]. The quantities $M_K(k_e, k_\nu)$ and $m_K(k_e, k_\nu)$ are the complicated expressions of different nuclear matrix elements (NMEs) and other kinematical factors.

The NMEs contains all the nuclear-structure information in the form

$$\begin{aligned} & [U]^{V/A} \mathcal{M}_{KLS}^{(N)}(pn)(k_e, m, n, \rho) \\ &= \frac{\sqrt{4\pi}}{\widehat{J}_i} \sum_{pn}^{V/A} m_{KLS}^{(N)}(pn)(k_e, m, n, \rho) (\Psi_f || [c_p^\dagger \tilde{c}_n]_K || \Psi_i). \end{aligned} \quad (7)$$

The nuclear matrix elements are divided into two parts: one part $^{V/A} m_{KLS}^{(N)}(pn)(k_e, m, n, \rho)$ is the single-particle matrix elements (SPMEs), which characterizes the properties of the transition operator and it is universal for all nuclear model. The SPMEs are calculated in the present work from the harmonic-oscillator wave functions [14, 17]. The second part $(\Psi_f || [c_p^\dagger \tilde{c}_n]_K || \Psi_i)$ is the one-body transition densities (OBTD) between initial (Ψ_i) and final (Ψ_f) nuclear states. The OBTDs contain the nuclear-structure information and they must be evaluated separately for each nuclear model. The summation runs over the proton (p) and neutron (n) single-particle states and the ‘‘hat-notation’’ reads $\widehat{J}_i = \sqrt{2J_i + 1}$.

3. Results and discussions

To calculate the one-body transition densities which are needed in the nuclear matrix elements, we have performed theoretical calculations in the framework of nuclear shell-model with KHH7B interaction. The KHH7B interaction consists of the model space covering the shell gap in the ranges $Z = 58 - 114$ and $N = 100 - 164$ around the ^{208}Pb . The model space includes the proton orbitals $1d_{5/2}$, $0h_{11/2}$, $1d_{3/2}$, and $2s_{1/2}$ below $Z = 82$ and the $0h_{9/2}$, $1f_{7/2}$, and $0i_{13/2}$ above, and the neutron orbitals $0i_{13/2}$, $2p_{3/2}$, $1f_{5/2}$, and $2p_{1/2}$ below $N = 126$ and the $1g_{9/2}$, $0i_{11/2}$, and $0j_{15/2}$ above. The orbitals used in this model space are shown in Fig. 1 with the experimental single particle/hole energies relative to ^{208}Pb . In KHH7B interaction, the cross shell two-body matrix elements (TBMEs) were generated by the G-matrix potential (H7B) [19], and

the proton-neutron hole-hole and particle-particle TBMEs are used from Kuo-Herling interaction [20] as modified in [21]. Previously, shell model results using KHH7B interaction are reported in Refs. [2, 3, 22, 23]. For the calculation, we have used the nuclear shell-model code OXBASH [24].

In Fig. 2, we have calculated the energy spectra of the ^{207}Tl and compared them with the experimental data. In the present calculations, we have correctly reproduced ground state $1/2^+$ in ^{207}Tl from the KHH7B interaction. The ground state $1/2^+$ and few excited states $3/2^+$, $11/2^-$, and $5/2^+$ are the single-particle states that we have calculated without excitations of particle. In Table 1, we have shown the dominant wave functions of the various low-lying energy states corresponding to $t = 0$ (no excitation) and $t = 1$ (for both protons and neutrons excitation) calculations. The single particle states $1/2^+$, $3/2^+$, $11/2^-$ and $5/2^+$ have reproduced corresponding to the single-proton-hole states $\pi s_{1/2}^{-1}$, $\pi d_{3/2}^{-1}$, $\pi h_{11/2}^{-1}$, and $\pi d_{5/2}^{-1}$, respectively, as we can see in the Table 1. In the β decay, a neutron in $N < 126$ orbitals of parent nucleus ^{207}Hg decaying into the $Z > 82$ orbitals in the daughter nucleus ^{207}Tl . In this situations, both the proton and neutron pairs are broken across the core ^{208}Pb to form the $2p-3h$ configurations in the final states, by making calculation with $1p-1h$ truncation for both protons and neutrons across the ^{208}Pb in the final state. Earlier, with this truncation, the high-spin states in ^{207}Tl are well-reproduced in Ref. [3]. The nucleon excitation across the core has large influence on the first-forbidden β decay nuclear matrix elements [7]. Mixing between the $t = 0$ and core excited configuration are blocked in our calculation for the energy spectra as shown in the Fig. 2.

Once the energy spectra are reasonably reproduced, then we have used the wave function to calculate the nuclear matrix elements needed in the β decay rate. We have considered the two main aspects in our calculations: First is the effective values of weak coupling constants and the second one is the effect of mesonic enhancement in the axial-charge matrix element γ_5 for the $\Delta J = 0$ transitions. First, we will discuss the quenching in the coupling constants that are playing an important role in the β decay rates. In the previous

Table 1: Dominant configurations of the states in ^{207}Tl with KHH7B interaction.

J^π	$E(\text{MeV})$	Dominant configuration	Probability%
$1/2^+$	0.000	$\pi s_{1/2}^{-1}$	100
$3/2^+$	0.351	$\pi d_{3/2}^{-1}$	100
$11/2_1^-$	1.348	$\pi h_{11/2}^{-1}$	100
$5/2^+$	1.683	$\pi d_{5/2}^{-1}$	100
$9/2_1^-$	2.756	$\pi s_{1/2}^{-2} \pi h_{9/2}$	61
$9/2_2^-$	2.927	$\pi s_{1/2}^{-1} \nu p_{1/2}^{-1} \nu g_{9/2}$	63
$11/2_2^-$	3.062	$\pi s_{1/2}^{-1} \nu p_{1/2}^{-1} \nu g_{9/2}$	44
$7/2_1^-$	3.130	$\pi s_{1/2}^{-1} \nu p_{3/2}^{-1} \nu g_{9/2}$	20
$7/2_2^-$	3.151	$\pi d_{3/2}^{-1} \nu p_{1/2}^{-1} \nu g_{9/2}$	35
$9/2_3^-$	3.222	$\pi s_{1/2}^{-1} \nu p_{1/2}^{-1} \nu g_{9/2}$	42
$11/2_3^-$	3.234	$\pi s_{1/2}^{-1} \nu p_{1/2}^{-1} \nu g_{9/2}$	35
$5/2_1^-$	3.264	$\pi d_{3/2}^{-1} \pi s_{1/2}^{-1} \pi h_{9/2}$	29
$9/2_4^-$	3.304	$\pi s_{1/2}^{-1} \nu p_{1/2}^{-1} \nu g_{9/2}$	35
$7/2_3^-$	3.455	$\pi d_{3/2}^{-1} \nu p_{1/2}^{-1} \nu g_{9/2}$	37
$11/2_4^-$	3.469	$\pi s_{1/2}^{-1} \nu p_{1/2}^{-1} \nu i_{11/2}$	51
$9/2_5^-$	3.481	$\pi d_{3/2}^{-1} \nu p_{1/2}^{-1} \nu g_{9/2}$	36
$5/2_2^-$	3.520	$\pi d_{3/2}^{-1} \nu p_{1/2}^{-1} \nu g_{9/2}$	58
$9/2_6^-$	3.523	$\pi d_{3/2}^{-1} \nu p_{1/2}^{-1} \nu g_{9/2}$	31
$7/2_4^-$	3.526	$\pi d_{3/2}^{-2} \pi h_{9/2}$	26
$9/2_7^-$	3.575	$\pi s_{1/2}^{-1} \nu p_{3/2}^{-1} \nu g_{9/2}$	20
$7/2_5^-$	3.646	$\pi s_{1/2}^{-1} \nu p_{3/2}^{-1} \nu g_{9/2}$	31
$9/2_8^-$	3.675	$\pi s_{1/2}^{-1} \nu p_{1/2}^{-1} \nu i_{11/2}$	32
$7/2_6^-$	3.690	$\pi d_{3/2}^{-1} \nu p_{1/2}^{-1} \nu g_{9/2}$	24
$5/2_3^-$	3.710	$\pi d_{3/2}^{-2} \pi h_{9/2}$	27
$9/2_9^-$	3.757	$\pi d_{3/2}^{-1} \pi s_{1/2}^{-1} \pi h_{9/2}$	20
$7/2_7^-$	3.802	$\pi s_{1/2}^{-1} \nu f_{5/2}^{-1} \nu g_{9/2}$	21
$9/2_{10}^-$	3.829	$\pi s_{1/2}^{-1} \nu f_{5/2}^{-1} \nu g_{9/2}$	53

Table 2: Comparison of the theoretical and experimental $\log ft$ values for the first-forbidden β^- transitions of ^{207}Hg ($9/2^+$) into the different excited states in ^{207}Tl . The experimental excitation energy, branching fractions, and $\log ft$ values are taken from [4].

J_f^π (Expt.)	J_f^π (SM)	E_i (MeV) (Expt.)	E_i (MeV) (SM)	Q (MeV)	β^- branching	$\log ft$	
						Expt.	SM
$11/2^-$	$11/2_1^-$	1.348	1.348	3.202	11(7)	7.2(4)	8.19
$7/2^-$	$7/2_1^-$	2.676	3.130	1.874	0.3(2)	7.8(3)	6.24
$5/2^-$	$5/2_1^-$	2.709	3.264	1.841	0.02(2)	>8.7	9.12
$(9/2^-)$	$9/2_1^-$	2.912	2.756	1.638	6(2)	6.3(2)	6.62
$(9/2^-)$	$9/2_2^-$	2.985	2.927	1.565	40(5)	5.42(7)	4.86
$(7/2^-)$	$7/2_2^-$	3.013	3.151	1.537	0.21(5)	7.7(2)	6.23
$(9/2^-)$	$9/2_3^-$	3.105	3.222	1.445	21(3)	5.58(8)	5.59
$(9/2^-)$	$9/2_4^-$	3.143	3.304	1.407	8(1)	5.95(7)	5.90
$(5/2^-)$	$5/2_2^-$	3.197	3.520	1.353	0.001(1)	>9.5	9.86
$(7/2^-)$	$7/2_3^-$	3.274	3.455	1.276	2.3(3)	6.34(8)	6.66
$(9/2^-)$	$9/2_5^-$	3.296	3.481	1.254	3.2(4)	6.17(8)	6.81
$(9/2^-)$	$9/2_6^-$	3.337	3.523	1.213	6.5(6)	5.81(7)	6.00
$(9/2^-)$	$9/2_7^-$	3.359	3.575	1.191	3.8(4)	6.01(7)	6.89
$(7/2^-)$	$7/2_4^-$	3.431	3.526	1.119	0.70(8)	6.65(8)	8.20
$(5/2^-, 7/2)$	$5/2_3^-$	3.494	3.710	1.056	0.0060(9)	8.63(9)	10.68
$(5/2^-, 7/2)$	$7/2_5^-$	3.494	3.646	1.056	0.0060(9)	8.63(9)	7.86
$(11/2)$	$11/2_2^-$	3.570	3.062	0.980	0.12(2)	7.21(10)	5.80
$(9/2^-)$	$9/2_8^-$	3.581	3.675	0.969	0.20(2)	6.97(8)	7.99
$(7/2^-)$	$7/2_6^-$	3.592	3.690	0.958	0.14(2)	7.11(9)	6.92
$(11/2^-)$	$11/2_3^-$	3.634	3.234	0.916	0.70(8)	6.34(8)	6.04
$(11/2^-)$	$11/2_4^-$	3.644	3.469	0.906	0.28(4)	6.72(9)	6.77
$(9/2, 11/2)$	$9/2_9^-$	3.800	3.757	0.750	0.041(5)	7.27(9)	7.94
$(9/2, 11/2)$	$11/2_5^-$	3.800	3.523	0.750	0.041(5)	7.27(9)	8.85
$(7/2, 9/2)$	$7/2_7^-$	3.850	3.802	0.700	0.022(6)	7.4(2)	6.38
$(7/2, 9/2)$	$9/2_{10}^-$	3.850	3.829	0.700	0.022(6)	7.4(2)	8.16
$(9/2, 11/2)$	$9/2_{11}^-$	3.940	3.876	0.610	0.031(4)	7.08(10)	7.86
$(9/2, 11/2)$	$11/2_6^-$	3.940	3.624	0.610	0.031(4)	7.08(10)	6.58

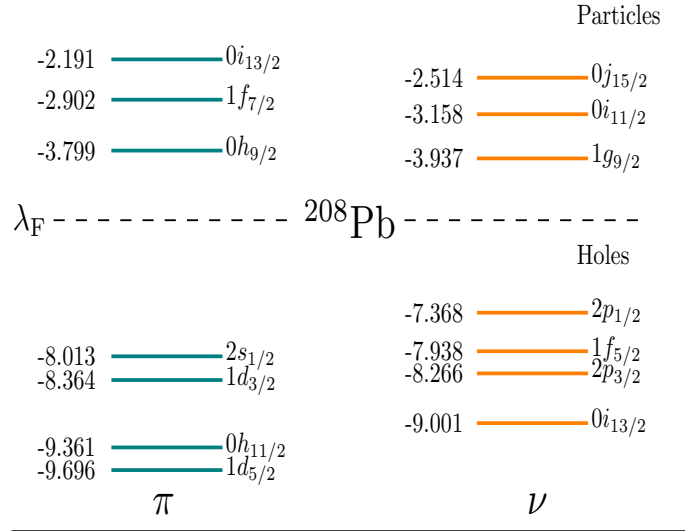
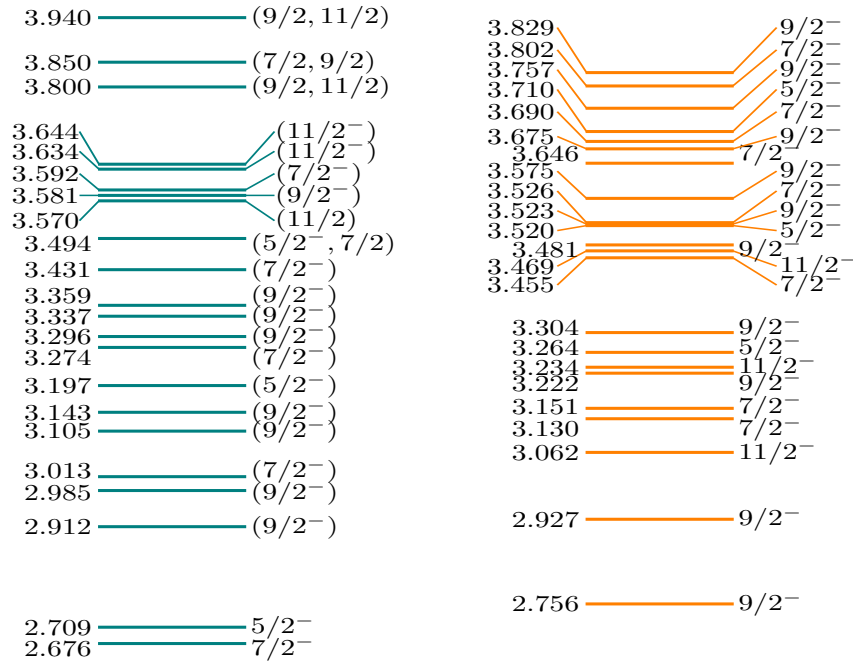


Figure 1: The model space with the experimental single-particle energies that are taken from the experiment energy spectra of $A = 207$ and 209 relative to ^{208}Pb .

study of the lead region, heavily quenched values of the coupling constants g_A and g_V for the first-forbidden β decay of 1^- transitions were suggested in Refs. [8, 7, 10, 11]. Warburton's calculation for the first-forbidden transitions in the lead region has found that the quenching factor in the coupling constants $g_A/g_A^{\text{free}} \approx 0.47$ and $g_V/g_V^{\text{free}} \approx 0.64$ [7]. Two set of quenching factors, $g_A/g_A^{\text{free}} = 0.34$, $g_V/g_V^{\text{free}} = 0.67$ and $g_A/g_A^{\text{free}} = 0.51$, $g_V/g_V^{\text{free}} = 0.30$ are calculated for the first-forbidden β^- decay of $^{205}\text{Tl}(1/2^+) \rightarrow ^{205}\text{Pb}(1/2^-)$ [25]. Recently, Zhi [11] et al., have performed the large-scale shell-model calculations for the number of nuclei around the magic numbers $N = 82, 126$ for both Gamow-Teller and first-forbidden β -decay and found that the quenching factor in coupling constants are $g_A/g_A^{\text{free}} = 0.38$ and $g_V/g_V^{\text{free}} = 0.51$. From this literature survey, it is concluded that the value of vector and axial-vector coupling constants are strongly quenched in the heavier mass region. This might be due to heavily truncated shell-model calculations in the heavier mass region.

The effect of the mesonic enhancement of the axial-charge matrix element γ_5 were studied in the lead region for several 0^- transitions and suggested the



^{207}Tl

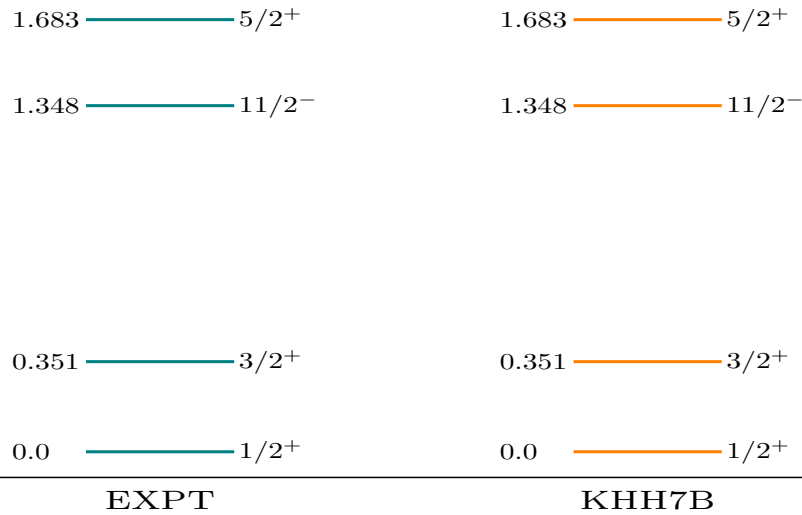


Figure 2: The shell-model results for the low-lying energy spectra for ^{207}Tl with KHH7B interaction in comparison with the experimental data.

value of enhancement factor $\epsilon_{\text{mec}} = 2.01 \pm 0.05$ that is about 100% of the impulse approximation [8]. For the further calculation of the $\log ft$ values, we have used recently calculated quenching factor of $g_A/g_A^{\text{free}}=0.38$ and $g_V/g_V^{\text{free}}=0.51$ by Zhi et al. [11] and along with this we have used the mesonic enhancement factor $\epsilon_{\text{mec}} = 2.01 \pm 0.05$ in the matrix element γ_5 for the 0^- transition [8].

To calculate the β decay rate, a precise Q value is needed. In our calculations, we have adopted the experimental $Q = 4.550$ MeV [26] value to calculate the $\log ft$ value for the β^- decay of ^{207}Hg . Our theoretical prediction for the $\log ft$ values of ^{207}Hg are compared with the recent experimental data [4] in Table 3 together with the experimental excitation energy of final states and Q values. The theoretical prediction of $\log ft$ values for the studied transition are not available in the literature. First time we have calculated the $\log ft$ from the nuclear shell-model by including the core polarization effect in the nuclear matrix elements. Our calculated $\log ft$ values are found in good agreement with the experimental data.

The state $11/2_1^-$ at 1.348 MeV has the single particle character that is reproduced by the one-proton-hole ($\pi h_{11/2}^{-1}$) configuration with 100% occupancy in $t = 0$ truncation. If we consider the $2p - 3h$ admixture in the $11/2_1^-$ for the β decay study then the $11/2_1^-$ is predicted with probability 83% $\pi h_{11/2}^{-1}$. In Table 3, we have reported the $\log ft$ value of 8.19 corresponding to the $11/2^-$ state with the configuration mixing in the final state, this is close to the experimental value of 7.2(4). On the other hand without excitation i.e. for $t = 0$ calculation, we have obtained the $\log ft$ value 8.52.

Our theoretical prediction of $\log ft$ values for the $5/2^-$ states at 2.709 MeV and 3.197 MeV are in reasonable agreement with the experimental data. These states could be a $5/2^-$ and obtained $\log ft$ values are 9.12 and 9.86 corresponding to energy value 2.709 MeV and 3.197 MeV, respectively, this is consistent with the unique first-forbidden decay. A state at 2.912 MeV is experimentally tentative ($9/2^-$), with $\log ft$ value 6.3(2). Our calculated $\log ft$ for $9/2_1^-$ is 6.62, which is in excellent agreement with the experimental data. The calculated $\log ft$ values for $9/2_3^-$ and $9/2_4^-$ are 5.59 and 5.90, respectively, corresponding

to the experimental values 5.58(8) and 5.95(7). For other $9/2^-$ states at 3.296, 3.337 and 3.359 MeV the calculated $\log ft$ values are in good agreement with the experimental data.

In Refs. [4, 22], they have experimentally populated new states ($5/2^-, 7/2^-$) at 3.494 MeV with the $\log ft$ value of 8.63(9), and this state is identical to $7/2^+$ at 3.474 MeV observed previously in [27]. In Ref. [22] the experimentally calculated $\log ft$ value for the 3.474 state is 8.53(9) and this is exactly predicted by the shell-model calculation with the $2p - 3h$ admixture. Transitions from $9/2^+$ of ^{207}Hg to ($5/2^-$ and $7/2^-$) of ^{207}Tl (3.494 MeV) are characterized as the first-forbidden unique and nonunique β^- decay, respectively. Thus we have performed two sets of calculations for $9/2^+ \rightarrow 7/2^-$ and $9/2^+ \rightarrow 5/2^-$ transitions, the calculated $\log ft$ values corresponding to the first-forbidden unique and nonunique β^- decay are 10.68 and 7.86, respectively. Here, the $\log ft$ values with the transition $9/2^+ \rightarrow 7/2^-$ (3.494 MeV) is more close to the experimental result. Also, our theoretical prediction of the $\log ft$ value for the transition $9/2^+ \rightarrow 5/2^-$ (3.494 MeV) is found to be consistent with the first-forbidden unique β decay.

The 3.570 MeV state is experimentally identified as the ($11/2^-$) with $\log ft$ value 7.21(10). The calculated $\log ft$ value for $11/2^-$ state is 5.80. It can be seen that this transition is predicted too fast as compared with the experimental data. The spin and parity of states at the 3.800, 3.850, and 3.940 MeV are not confirmed from the experimental side. In Ref. [4], they have given some predictions of spin only at these energies with $\log ft$ values. Hence, we have calculated the $\log ft$ values for these three states from the nuclear shell-model corresponding to $9/2^-$ and $11/2^-$ states at 3.800 MeV, $7/2^-$ and $9/2^-$ states at 3.850 MeV and $9/2^-$ and $11/2^-$ states at 3.940 MeV. So our theoretical prediction could be useful for future experiments to confirm the spin and parity of these three states at 3.800, 3.850, and 3.940 MeV. In general, the computed $\log ft$ values for all the studied transitions are in good agreement with the experimental data. The calculated $11/2^-$ states corresponding to experimental state at 3.570, 3.634, 3.644, 3.800 and 3.940 MeV are at 3.062, 3.234, 3.469,

3.523 and 3.624 MeV, respectively.

From the comparison of the experimental and the shell model results, the octupole states are not well reproduced. Because the model space of KHH7B is too small for collective octupole states. This explains the lower predicted $\log ft$ values for the lowest energy $5/2^-$ and $7/2^-$ states. Maybe if we use KHM3Y interaction developed for a model space containing 24 orbitals [1], then it will be possible to reproduce octupole states in our calculation.

4. Conclusions

In this work, we have performed the shell-model calculations for the $\log ft$ values using KHH7B interaction for the first-forbidden β^- transitions corresponding to recently available experimental data [4]. In these calculations, we have used the $2p-3h$ admixture in the final state to include the core polarization effects in the β decay study. First, to test the predictive power of the used Hamiltonian, we have calculated the energy spectrum. After that, we have used the wave function in the calculation of the nuclear matrix elements that are needed in the β decay rate calculations. Also, we consider the mesonic enhancement factor $\epsilon_{\text{mec}} = 2.01 \pm 05$ in the axial-charge matrix element γ_5 and the quenching factor in coupling constants suggested in the literature in the lead region. First time we have calculated the $\log ft$ values from the shell-model with well-known interaction and found a reasonable agreement with the recent experimental data. We have also given the prediction of some unknown states based on the calculated $\log ft$ values. Our predictions might be very useful as input for future experiment. It is also noticed that calculated energy spectra for high-spin states are compressed thus further theoretical calculations with more particle excitations are needed to reproduce the collectivity and achieve convergence in the energy spectra for these states.

ACKNOWLEDGMENTS

A. K. would like to thank the Ministry of Human Resource Development (MHRD), Government of India, for the financial support for his thesis work. P.C.S. acknowledges a research grant from SERB (India), CRG/2019/000556. We would like to thank Prof. Zs. Podolyák for several useful discussions in this work.

References

- [1] B. A. Brown, “Double-octupole states in ^{208}Pb ”, *Phys. Rev. Lett.* **85**, 5300 (2000).
- [2] Zs. Podolyák *et al.*, “Octupole transitions in the ^{208}Pb region”, *J. Phys.: Conf. Ser.* **580**, 012010 (2015).
- [3] E. Wilson *et al.*, “Core excitations across the neutron shell gap in ^{207}Tl ”, *Phys. Lett. B* **747**, 88 (2015).
- [4] T. A. Berry *et al.*, “Octupole states in ^{207}Tl studied through β decay”, *Phys. Rev. C* **101**, 054311 (2020).
- [5] I. E. Alekseev *et al.*, “Precision measurement of the ^{210}Bi β spectrum”, *Phys. Rev. C* **102**, 064329 (2020).
- [6] R. J. Carroll *et al.*, “Competition between allowed and first-forbidden β decay: the case of $^{208}\text{Hg} \rightarrow ^{208}\text{Tl}$ ”, *Phys. Rev. Lett.* **125**, 192501 (2020).
- [7] E. K. Warburton, “Core polarization effects on spin-dipole and first-forbidden β -decay operators in the lead region”, *Phys. Rev. C* **42**, 2479 (1990).
- [8] E. K. Warburton, “First-forbidden β decay in the lead region and mesonic enhancement of the weak axial current”, *Phys. Rev. C* **44**, 233 (1991).
- [9] E. K. Warburton, “Mesonic enhancement of the weak axial-vector current evaluated from β decay in lead region”, *Phys. Rev. Lett.* **66**, 1823 (1991).

- [10] T. Suzuki, T. Yoshida, T. Kajino, and T. Otsuka, “ β decays of isotones with neutron magic number of $N = 126$ and r -process nucleosynthesis”, *Phys. Rev. C* **85**, 015802 (2012).
- [11] Q. Zhi, E. Caurier, J. J. Cuenca-García, K. Langanke, G. Martínez-Pinedo and K. Sieja, “Shell-model half-lives including first-forbidden contributions for r -process waiting-point nuclei”, *Phys. Rev. C.* **87**, 025803 (2013).
- [12] S. J. Haselschwardt, J. Kostensalo, X. Mougeot, and J. Suhonen, “Improved calculations of β decay backgrounds to new physics in liquid xenon detectors”, *Phys. Rev. C* **102**, 065501 (2020).
- [13] M. Brunet et al., ”Competition between allowed and first-forbidden β decays of ^{208}At and expansion of the ^{208}Po level scheme”, *Phys. Rev. C* **103**, 054327 (2021).
- [14] M. Haaranen, J. Kotila, and J. Suhonen, “Spectrum-shape method and the next -to-leading-order terms of the β -decay shape factor”, *Phys. Rev. C* **95**, 024327 (2017).
- [15] H. Behrens and W. Bühring, *Electron Radial Wave Functions and Nuclear Beta-Decay* (Clarendon Press, 1982).
- [16] C. Patrignani and Particle Data Group, “Review of Particle Physics”, *Chinese Phys. C* **40**, 100001 (2016).
- [17] M. T. Mustonen, M. Aunola, and J. Suhonen, “Theoretical description of the fourth-forbidden non-unique β decays of ^{113}Cd and ^{115}In ”, *Phys. Rev. C* **73** 054301 (2006); Erratum *Phys. Rev. C* **76**, 019901 (2007)
- [18] A. Kumar, P. C. Srivastava, J. Kostensalo and J. Suhonen, “Second-forbidden nonunique β^- decays of ^{24}Na and ^{36}Cl assessed by the nuclear shell-model”, *Phys. Rev. C.* **101**, 064304 (2020).

- [19] A. Hosaka, K.-I. Kubo, and H. Toki, “G-matrix effective interaction with the paris potential” Nucl.Phys. A **444**, 76 (1985).
- [20] T. T. S. Kuo and G. H. Herling, Report No. 2258, US Naval Research Laboratory, 1971, unpublished.
- [21] E. K. Warburton and B. A. Brown “Appraisal of the Kuo-Herling shell-model interaction and application to $A = 210 - 212$ nuclei”, Phys. Rev. C **43**, 602 (1991).
- [22] T. A. Berry *et al.*, “Investigation of the $\Delta n = 0$ selection rule in Gamow-Teller transitions: The β -decay of ^{207}Hg ”, Phys. Lett. B **793**, 271 (2019).
- [23] S.G. Wahid *et al.*, Metastable states from multinucleon excitations in ^{202}Tl and ^{203}Pb , Phys.Rev. C **103** , 024329 (2020).
- [24] B. A. Brown et al., ”OXBASH for Windows”, MSU-NSCL report 1289, 2004.
- [25] L. Rydström, J. Blomqvist, R. J. Liotta, and C. Pomar, “Structure of proton-deficient nuclei near ^{208}Pb ”, Nucl. Phys. A. **512**, 217 (1990).
- [26] M. Wang, G. Audi, F. G. Kondev, W. J. Huang, S. Naimi, and X. Xu, “The AME2016 atomic mass evaluation”, Chin. Phys. C **41**, 030003 (2017).
- [27] F. G. Kondev, and S. Lalkovski, “Nuclear Data Sheets for A=207”, Nucl. Data Sheets **112**, 707 (2011).